

Experimental Performance of Pilot-Oxygen-Pressure Swing Adsorption Unit

Radek Šulc*, Miroslav Kos

Czech Technical University in Prague, Faculty of Mechanical Engineering, Department of Process Engineering, Technická 4, 160 00, Prague 6, Czech Republic
 Radek.Sulc@fs.cvut.cz

The effect of product purity on product flowrate, oxygen recovery, adsorbent productivity, and specific energy demand was investigated for the adsorption pressure of 5.5 bar (g). The experiments were carried out for zeolite molecular sieve UOP MOLSIV™ PSAO2 XP (UOP LLC, Honeywell) with N₂/O₂ enhanced selectivity in the pilot-plant adsorption unit using two-bed pressure swing adsorption technology. The oxygen recovery, adsorbent productivity, and specific energy demand were found in the range of 0.44 to 0.32, from 205 to 286 kg tO₂⁻¹ d, and from 0.556 to 0.767 kWh NmO₂⁻³, respectively, for oxygen purity in the product stream increasing from 89 to 94.7 %.

1. Introduction

The Pressure Swing Adsorption (PSA) units are widely used as an oxygen source where oxygen is produced in gaseous form. The start-up time of minutes is an undeniable advantage of PSA technology compared to cryogenic air separation, which has a start-up time of hours or days. Nitrogen-selective zeolites 5A and 13X are the most commonly used for oxygen separation from the air (Chin et al., 2023). Using nitrogen-selective zeolites, the oxygen content in the product gas is limited to 95 %. The rest of the product stream is mainly argon. The composition of the exhaust gas is approximately 85 – 90 % nitrogen and 10 – 15 % oxygen (Banaszkiewicz and Gizicki, 2020). Argon-oxygen selective silver-modified X-zeolites or carbon molecular sieves are used as adsorbents (Santos et al., 2007) to obtain higher oxygen purity. To this day, lithium-doped silica zeolites (Li-SLX) are considered the best adsorbents for PSA/VPSA oxygen production (Chin et al., 2023). Today, zeolites modified by a single cation (Yang et al., 2019) or mixed cations (Epiepang et al., 2019) are investigated as potentially better alternatives.

Zhu et al. (2017) developed a novel rapid vacuum pressure swing adsorption process (RVPSA) with intermediate gas pressurization for oxygen production. For 90 % oxygen purity, they reported 29.45 % oxygen recovery and a bed size factor of 82.84 kg tO₂⁻¹ d for the adsorption and desorption pressures of 240 kPa and 60 kPa, respectively. The Li-LSX was used as an adsorbent. Banaszkiwicz and Chorowski (2018) experimentally analysed the dependence of energy consumption on oxygen purity in a mobile pilot unit utilizing vacuum-pressure-temperature swing adsorption Technology (VPTSA) for air separation. They found energy consumption of 892 kWh tO₂⁻¹ for oxygen of 94 % oxygen purity. Gizicki and Banaszkiwicz (2020) analyzed experimentally energy consumption with the use of a commercially available oxygen-PSA generator using 5A zeolite. They reported an energy consumption of 1,450-1,530 kWh t⁻¹ for the adsorption pressure of 5.5 bar (g) and 95 % oxygen.

The effect of product purity on product flowrate, oxygen recovery, adsorbent productivity, and specific energy demand was investigated for the adsorption pressure of 5.5 bar (g) in the pilot-plant adsorption unit using zeolite molecular sieve UOP MOLSIV™ PSAO2 XP (UOP LLC, Honeywell) with N₂/O₂ enhanced selectivity.

1.1 Experimental set-up

The pilot plant adsorption unit O2 (manufactured by OXYWISE Ltd., Slovakia) was used to carry out all the experiments. The adsorption unit utilizes two-bed Pressure Swing Adsorption technology. The nominal capacity

of this unit is 1.3 kg/h of gaseous oxygen with a purity of 95 % oxygen. The PSA units require an inlet air quality of class 1.4.1 (solid particles, air humidity, oil). It is necessary to treat compressed air to achieve air quality. A refrigeration air drying produces an air of the required pressure dew point of +3 °C. The adsorption unit schema is shown in Figure 1a. The parameters of the main components are described in Šulc and Kos (2022) in detail. The experiments were carried out for the porous zeolite molecular sieve UOP MOLSIIV™ PSAO2 XP (UOP LLC, Honeywell) with N₂/O₂ enhanced selectivity. Adsorbent particles are homogeneous spheres of 2 mm diameter (8×12 mesh) with a bulk density of 656.8 kg/m³. The adsorbent properties are presented in Table 1. The weight of the adsorbent in the column was approximately 8.69 kg. The standard cycle consists of these sequential steps: 1) equalization, 2) pressurization, 3) production, 4) equalization, and 5) purging. At present, the industrially used cycles combine pressurization and production steps, as demonstrated in Figure 1b. The following time intervals were used for the experiment: i) 48 s for the pressurization, ii) 19 s for the equalization, and iii) 24 s for the production step.

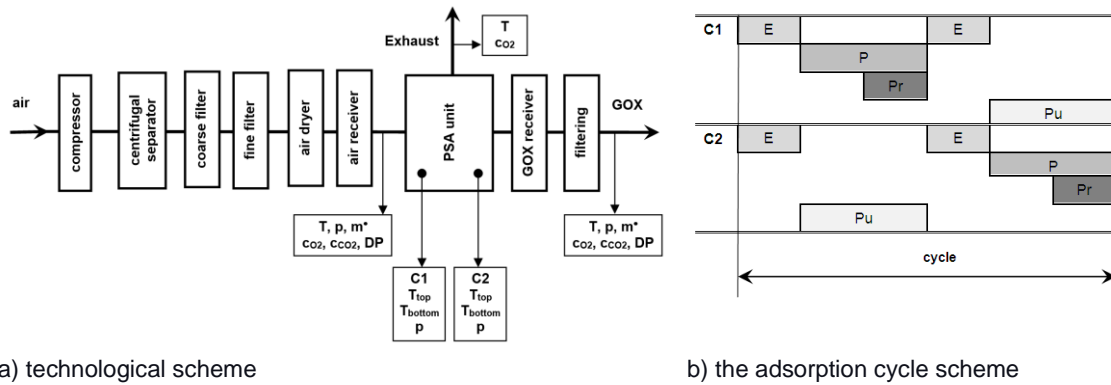


Figure 1: Pilot-plant adsorption unit: a) the technological scheme, b) the scheme of the adsorption cycle used for columns C1 and C2: E-equalization, P-pressurization, Pr-production, and Pu-purging

Table 1: Properties of UOP MOLSIIV™ PSAO2 XP

Particle diameter (m)	BET surface area (m ² g ⁻¹)	Outer surface area (m ² g ⁻¹)	Micropore area (m ² g ⁻¹)	Pore volume (m ³ g ⁻¹)	Micropore volume (m ³ g ⁻¹)	Particle porosity (-)	Bulk density (kg m ⁻³)	Particle density (kg m ⁻³)
0.002	522.8	40.2	246.7	3.47×10 ⁻⁴	2.47×10 ⁻⁴	0.38	678.96	1095.1

1.2 Experimental data

The mass gas flow rate, the volumetric concentrations of oxygen and CO₂, and the dew point were measured in the air and product gas streams for the adsorption pressure of 5.5 bar (g). The oxygen flowrate in the product stream was changed in the range from 1.4 to 2.0 kg h⁻¹ using the product stream regulation valve. A total of 13 datasets were recorded.

Each dataset lasts approximately 23 minutes. For each selected oxygen flowrate, the data set was recorded in a steady state. The mean mass flowrate was calculated using internal integration built into the flowmeter for each dataset as follows:

$$\overline{MF} = (TM_2 - TM_1)/(t_2 - t_1), \quad (1)$$

where TM₁ (t₁) and TM₂ (t₂) are the total weights recorded by the flowmeter at the beginning and the end of the dataset respectively. The mean values of the other measured quantities such as oxygen content, dew point, temperature, etc. were calculated by averaging instantaneous values recorded by sensors. The calculated mean values of the selected measured quantities are presented in Table 2.

Table 2: Experimental data – mean values evaluated

Dataset No.	Oxygen content (% mol.)			Mass flowrate (kg h ⁻¹)		CO ₂ content (ppm)		Dew point (°C)	
	Air	Product stream	Exhaust stream	Air	Product stream	Air	Product stream	Air	Product stream
1	21.04	94.65	16.76	17.1	1.35	577	0.2	-0.8	-79.2
2	21.04	94.5	16.3	17.4	1.45	521	0.06	-0.9	-79.3
3	21.04	94.55	15.89	17.6	1.5	518	0.11	-1.0	-79.0
4	21.04	94.38	15.29	17.5	1.55	525	0.11	-1.0	-79.5
5	21.04	94.46	15.46	17.6	1.55	522	0.09	-1.1	-79.0
6	21.04	94.31	14.86	17.6	1.59	508	0.11	-1.1	-79.4
7	21.04	94.05	14.64	17.3	1.6	532	0.17	-1.0	-78.7
8	21.09	93.29	13.53	17.2	1.7	531	0.23	-1.0	-79.1
9	21.05	93.56	13.76	17.4	1.71	548	0.18	-1.1	-79.0
10	21.09	91.97	12.59	17.3	1.82	527	0.23	-1.1	-79.1
11	21.08	91.99	12.63	17.1	1.79	519	0.28	-0.8	-78.9
12	21.07	90.98	12.03	17.3	1.87	519	0.23	-1.0	-78.6
13	21.05	89.44	11.62	17.4	1.99	531	0.11	-1.0	-79.2

2. Results and Discussion

2.1 Product stream composition

The following quantities are usually measured in the product stream: i) oxygen content, ii) CO₂ content, and iii) water content. The question arises as to what is the remaining content of the product stream. As reported in the literature, using nitrogen-selective zeolites (type A and type X zeolites), the oxygen purity is limited to 95% oxygen in the product stream and the rest of the product stream is mainly argon. The composition of the product stream is usually not fully presented. Beeyani et al. (2010) modelled the PSA process assuming that the proportion between argon and oxygen is the same both in the air stream and in the product stream, i.e.

$$\frac{\dot{n}_{Ar-air}}{\dot{n}_{O_2-air}} = \frac{\dot{n}_{Ar-product}}{\dot{n}_{O_2-product}}, \quad (2)$$

Eq. (2) can be rearranged as follows:

$$y_{Ar-product} = \frac{y_{Ar-air}}{y_{O_2-air}} \cdot y_{O_2-product}, \quad (3)$$

where y_{Ar} (-) and y_{O_2} (-) are mole fractions of argon and oxygen, respectively, in the air stream or the product stream. Thus, with an increase in the product stream flowrate, the concentration of argon and oxygen will decrease in the same manner in the product stream as the nitrogen manages to break the adsorption bed into the product stream. This assumption was based on the known fact that the sorption isotherms for argon and oxygen are the same for zeolite molecular sieves as reported by Yang (2003). Therefore, two hypotheses were tested: i) the product stream contains only oxygen and argon (noted Hypothesis No. 1), and ii) the product stream contains the same proportion of oxygen and argon as in the air stream (noted Hypothesis No. 2). The mass balance was performed under the following two assumptions: i) the water content was neglected in all streams, and ii) the CO₂ content in the product gas was omitted owing to its negligible concentration. The calculated composition of the product stream and the exhaust stream is presented in Table 3 and Table 4 for both hypotheses.

The argon content was found to be the best quantity for the hypothesis assessment. Assuming that there is no nitrogen in the product stream, the argon content calculated in the product stream for oxygen purity less than 90 % reached the negative value which is meaningless. Therefore, the postulate proposed by Beeyani et al. (2010) seems to be more reliable than the postulate anticipating the presence of oxygen and argon in the product stream only.

On the other side, it should be noted that the oxygen content calculated in the exhaust stream varied in the range from 1.4 to 12 % from the measured value for both hypotheses.

Table 3: Stream composition – hypothesis No. 1^{*1}

Dataset No.	Product stream			Exhaust stream						
	oxygen ^{*2} (% mol.)	nitrogen ^{*3} (% mol.)	argon ^{*3} (% mol.)	oxygen ^{*2} (% mol.)	oxygen ^{*3} (% mol.)	relative error ^{*4} (%)	nitrogen ^{*3} (% mol.)	argon ^{*3} (% mol.)	CO ₂ ^{*3} (ppm)	
1	94.65	0	5.35	16.76	15.47	8.3	83.87	0.6	621	
2	94.5	0	5.50	16.30	15.14	7.7	84.24	0.56	563	
3	94.55	0	5.45	15.89	14.96	6.3	84.43	0.56	561	
4	94.38	0	5.62	15.29	14.77	3.5	84.64	0.53	570	
5	94.46	0	5.54	15.46	14.81	4.4	84.6	0.54	566	
6	94.31	0	5.69	14.86	14.62	1.6	84.81	0.51	553	
7	94.05	0	5.95	14.64	14.48	1.1	84.98	0.48	580	
8	93.29	0	6.71	13.53	14.14	-4.3	85.43	0.37	582	
9	93.56	0	6.44	13.76	14.09	-2.3	85.45	0.4	600	
10	91.97	0	8.03	12.59	13.81	-8.8	85.93	0.2	581	
11	91.99	0	8.01	12.63	13.8	-8.4	85.94	0.2	573	
12	90.98	0	9.02	12.03	13.63	-11.8	86.24	0.07	574	
13	89.44	0	10.56	11.62	13.4	-13.3	86.24	-0.15	591	

Note: ^{*1} Argon content of 0.93 mol % in dry air. ^{*2} Measured value. ^{*3} Calculated value. ^{*4} Related to the calculated value.

Table 4: Stream composition – hypothesis No. 2^{*1}

Dataset No.	Product stream			Exhaust stream						
	oxygen ^{*2} (% mol.)	nitrogen ^{*3} (% mol.)	argon ^{*3} (% mol.)	oxygen ^{*2} (% mol.)	oxygen ^{*3} (% mol.)	relative error ^{*4} (%)	nitrogen ^{*3} (% mol.)	argon ^{*3} (% mol.)	CO ₂ ^{*3} (ppm)	
1	94.65	1.16	4.18	16.76	15.45	8.5	83.81	0.68	621	
2	94.5	1.33	4.18	16.30	15.11	7.9	84.17	0.67	563	
3	94.55	1.27	4.18	15.89	14.93	6.5	84.36	0.66	561	
4	94.38	1.45	4.17	15.29	14.73	3.8	84.56	0.65	570	
5	94.46	1.37	4.17	15.46	14.77	4.7	84.52	0.65	566	
6	94.31	1.53	4.17	14.86	14.58	1.9	84.72	0.64	553	
7	94.05	1.79	4.16	14.64	14.43	1.4	84.87	0.64	580	
8	93.29	2.6	4.11	13.53	14.07	-3.8	85.25	0.62	582	
9	93.56	2.31	4.13	13.76	14.02	-1.9	85.3	0.62	601	
10	91.97	3.98	4.06	12.59	13.69	-8.0	85.65	0.6	582	
11	91.99	3.95	4.06	12.63	13.68	-7.6	85.66	0.6	574	
12	90.98	5	4.02	12.03	13.48	-10.8	85.87	0.6	575	
13	89.44	6.61	3.95	11.62	13.19	-11.9	86.17	0.58	592	

Note: ^{*1} Argon content of 0.93 mol % in dry air. ^{*2} Measured value. ^{*3} Calculated value. ^{*4} Related to the calculated value.

2.2 Air factor, oxygen recovery, and adsorbent productivity

Some manufacturers of oxygen PSA generators use the term 'air factor'. The air factor is the air ratio defined as the ratio of the air flowrate at the PSA inlet to the gaseous oxygen stream that is produced (GOX), i.e. product gas:

$$AirF = \dot{V}_{air}^N / \dot{V}_{GOX}^N, \quad (4)$$

where AirF is the air ratio (Nm³ Nm⁻³), \dot{V}_{air}^N is the volumetric airflow rate at the PSA unit inlet under standard conditions (Nm³ s⁻¹), \dot{V}_{GOX}^N is the volumetric flowrate of the gaseous oxygen stream (GOX) produced by the PSA unit under standard conditions (Nm³ s⁻¹).

The oxygen recovery is defined as the ratio of the oxygen flowrate in the air entering the PSA unit to the oxygen flowrate in the product stream (GOX):

$$R_{O_2} = \frac{\dot{n}_{O_2-product}}{\dot{n}_{O_2-air}} = \frac{y_{O_2-product} \cdot \dot{n}_{product}}{y_{O_2-air} \cdot \dot{n}_{air}} = \frac{y_{O_2-product}}{y_{O_2-air}} \cdot \frac{1}{AirF}, \quad (5)$$

where $y_{O_2-product}$ is the mole fraction of oxygen in the product stream (-), $\dot{n}_{product}$ is the molar flowrate of the product stream (kmol s⁻¹), y_{O_2-air} is the mole fraction of oxygen in the air fed to the PSA unit (-), and \dot{n}_{air} is the

molar air flowrate (kmol s^{-1}). The adsorbent productivity is characterized by the bed size factor which is defined as the ratio of adsorbent weight to the oxygen flow in the product stream (GOX):

$$BSF = \frac{m_{\text{adsorbent}}}{\dot{m}_{\text{O}_2\text{-product}}} = \frac{m_{\text{adsorbent}}}{M_{\text{O}_2} \cdot y_{\text{O}_2\text{-product}}} \cdot \frac{\text{Air}F}{(\dot{V}_{\text{air}}^N / 22.4)}, \quad (6)$$

where BSF is the bed size factor ($\text{kg}_{\text{adsorbent}} \text{kg}_{\text{O}_2}^{-1} \text{d}$), M_{O_2} is the molar weight of oxygen (kg kmol^{-1}), and \dot{V}_{air}^N is the volumetric airflow rate at the PSA unit input under standard conditions ($\text{Nm}^3 \text{d}^{-1}$). The calculated values for air factor and oxygen recovery are presented in Table 5 for each dataset.

Table 5: Process characteristics – air factor, oxygen recovery, and specific energy demand²

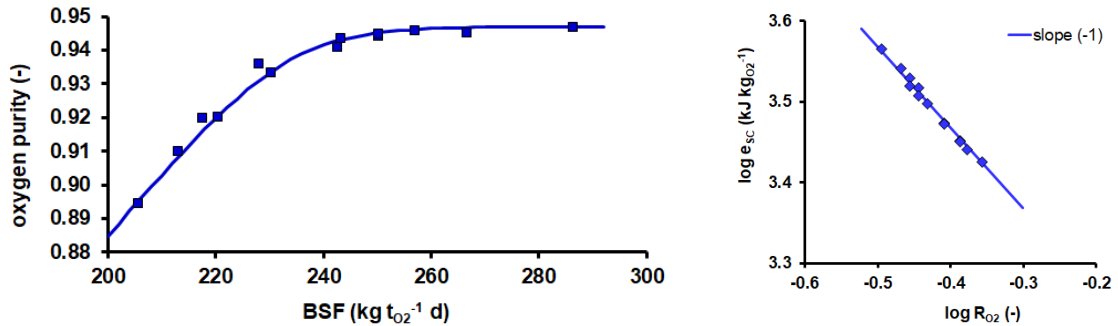
Dataset No.	Oxygen purity ^{*1} (% mol.)	Air factor (kmol kmol^{-1})	Oxygen recovery (-)	Specific energy demand ($\text{kJ kg}_{\text{O}_2}^{-1}$)	($\text{kWh Nm}_{\text{O}_2}^{-3}$) ^{*3}
1	94.65	14.2	0.32	3,675	0.767
2	94.5	13.4	0.34	3,478	0.726
3	94.55	13	0.35	3,384	0.707
4	94.38	12.6	0.36	3,287	0.686
5	94.46	12.7	0.35	3,306	0.69
6	94.31	12.3	0.36	3,214	0.671
7	94.05	12	0.37	3,147	0.657
8	93.29	11.3	0.39	2,972	0.621
9	93.56	11.3	0.39	2,971	0.62
10	91.97	10.6	0.41	2,828	0.591
11	91.99	10.6	0.41	2,825	0.59
12	90.98	10.2	0.42	2,759	0.576
13	89.44	9.7	0.44	2,663	0.556

Note: ^{*1} Oxygen content in the product stream. ^{*2} Data calculated for the mass balance obtained by hypothesis No. 2. ^{*3} Conversion factor: $1 \text{ kJ kg}_{\text{O}_2}^{-1} = 2.088 \cdot 10^{-4} \text{ kWh Nm}_{\text{O}_2}^{-3}$.

The effect of bed size factor air ratio on oxygen purity was evaluated as follows:

$$O_2 \text{ purity}(\%) = 100 \cdot \left[(0.0926 \cdot BSF^{0.426})^{-70} + (0.947)^{-70} \right]^{-1/70} \quad (7)$$

where O_2 purity is oxygen purity in the product gas (GOX), and BSF is the bed size factor ($\text{kg}_{\text{adsorbent}} \text{t}_{\text{O}_2}^{-1} \text{d}$). The comparison of experimental data and the proposed correlation is presented in Figure 2a.



a) bed size factor

b) specific energy demand

Figure 2: Process characteristics: a) bed size factor, b) specific energy demand

2.3 Specific energy demand

The specific energy demand ($\text{kJ kg}_{\text{O}_2}^{-1}$) was calculated as follows:

$$e_{sc} = \frac{P_c}{\dot{m}_{\text{O}_2\text{-product}}} = \frac{1}{\eta_c} \cdot p_1 \cdot \dot{V}_{\text{air}1} \cdot \frac{\kappa}{\kappa-1} \cdot \left[1 - \left(\frac{p_2}{p_1} \right)^{(\kappa-1)/\kappa} \right] \cdot \frac{1}{\dot{m}_{\text{O}_2\text{-product}}}, \quad (8)$$

where P_c is compressor electrical power input (kW), $m^{\bullet}_{O_2\text{-product}}$ is the oxygen flowrate in the product gas (kg s^{-1}), η_c is the overall compressor efficiency, p_1 is the inlet air pressure (kPa), $V^{\bullet}_{\text{air}1}$ is the air flowrate ($\text{m}^3 \text{s}^{-1}$) at inlet conditions (temperature t_1 , pressure p_1), p_2 is the outlet air pressure (kPa), κ is Poisson constant (-). The specific energy consumption was calculated for an air intake temperature of 20°C and pressure of 101.325 kPa, and outlet pressure of 650 kPa, $\kappa = 1.4$, $\eta_c = 0.76$. The overall compressor efficiency was estimated using datasheet data for the Kaeser compressor (Kaeser Kompressoren, 2022). For the e_{sc} calculation, the pressure losses were neglected and compression work was only taken into account. The calculated e_{sc} values are presented in Table 5 for each dataset. As expected, when the energy losses on the valves are omitted, the specific energy consumption needed for the product separation is inversely proportional to the oxygen recovery, as evidenced in Figure 2b. The specific energy demand estimated for the 94 % oxygen purity is comparable with the results presented by Banaszkiwicz and Chorowski (2018) for the VPTSA technology. The specific energy demand estimated for 95 % purity is approximately 1/3 less compared to data for 5A zeolite presented by Gizicki and Banaszkiwicz (2020) for the same adsorption pressure.

3. Conclusions

The effect of product purity on product flowrate, oxygen recovery, adsorbent productivity, and specific energy demand was investigated for the adsorption pressure of 5.5 bar (g) in the pilot-plant adsorption unit using two-bed pressure swing adsorption technology. The oxygen recovery, adsorbent productivity, and specific energy demand were found in the range of 0.44 to 0.32, from 205 to 286 $\text{kg O}_2\text{-}^1 \text{d}$, and from 0.556 to 0.767 $\text{kWh NmO}_2\text{-}^3$, respectively, for oxygen purity in the product stream increasing from 89 to 94.7 %. The specific energy demand estimated for 95 % purity is approximately 1/3 less compared to data for 5A zeolite presented by Gizicki and Banaszkiwicz (2020) for the same adsorption pressure. This finding confirms the expected better performance of UOP MOLSIV™ PSAO2 XP (UOP LLC, Honeywell) with N_2/O_2 enhanced selectivity. The estimated specific energy demand for 94 % oxygen purity is comparable with the results presented by Banaszkiwicz and Chorowski (2018) for the VPTSA technology. Simultaneously, the two hypotheses regarding product stream composition were tested. The assumption proposed by Beeyani et al. (2010) seems to be more reliable than the postulate anticipating the presence of oxygen and argon in the product stream only.

Acknowledgements

This work was supported by the Ministry of Education, Youth and Sports of the Czech Republic under OP RDE grant number CZ.02.1.01/0.0/0.0/16_019/0000753 "Research centre for low-carbon energy technologies". The authors thank Karel Soukup's Lab (ICPF, Czech Academy of Science) for the adsorbent sample analysis.

References

- Banaszkiwicz T., Chorowski M., 2018, Energy consumption of air-separation adsorption methods. *Entropy* 20, 232.
- Beeyani A., Singh K., Vyas R., Kumar S, Kumar S., 2010, Parametric studies and simulation of PSA process for oxygen production from air, *Polish Journal of Chemical Technology*, 12(2), 18-28.
- Chin C., Kamin Z., Vai Bahrun M.H., Bono A., 2023, The production of industrial-grade oxygen from air by pressure swing adsorption, *International Journal of Chemical Engineering*, 2023, 2308227.
- Epiepang F. E., Yang X., Li J., Wei Y., Liu Y., Yang R. T., 2019, Air separation sorbents: mixed-cation zeolites with minimum lithium and silver, *Chemical Engineering Science*, 198, 43–51.
- Gizicki W., Banaszkiwicz T., 2020, Performance Optimization of the Low-Capacity Adsorption Oxygen Generator, *Applied Sciences*, 10, 7495.
- Kaeser Kompressoren Ltd., 2023. datasheet "Rotary screw compressors, SX series. <<https://www.kaeser.com/int-en/products/rotary-screw-compressors/rotary-screw-compressors-with-fluid-cooling/compressed-air-supply-stations/premium-models>> accessed 9.02.2023.
- Santos J.C., Cruz P., Regala T., Magalhães F.D., Mendes A., 2007. High-purity oxygen production by pressure swing adsorption. *Ind. Eng. Chem. Res.* 46, 591-599.
- Šulc R., Kos M., 2022, Experimental Study of Oxygen Separation in Oxygen- Pressure Swing Adsorption Unit, *Chemical Engineering Transactions*, 94, 481-486.
- Yang R., 2003, *Adsorbents: Fundamentals and Applications*. Wiley, New Jersey, USA.
- Yang X., Epiepang F.E., Li J., Wei Y., Liu Y., Yang R.T., Sr-LSX zeolite for air separation, 2019, *Chemical Engineering Journal*, 362, 482-486.
- Zhu X., Liu Y., Yang, X., Liu W., 2017, Study of a novel rapid vacuum pressure swing adsorption process with intermediate gas pressurization for producing oxygen, *Adsorption*, 23, 175-184.